Electronic Supplementary Material (ESI) for Journal of Materials Chemistry B.

Supporting Information For

NIR light-driving aza-BODIPY with two efficacy fragments for photothermal therapy by triggering cancer cell apoptosis

Chunyu Shao,[a†] Xiuyan Gong,[b†] Dongxiang Zhang,[a] Xin-Dong Jiang,*[a] Jianjun Du*[c] and Guiling Wang*[b]

[a] Liaoning & Shenyang Key Laboratory of Functional Dye and Pigment, Shenyang University of Chemical Technology, Shenyang, China. E-mail:xdjiang@syuct.edu.cn

[b] Department of Cell Biology, China Medical University, Shenyang, 110122, China. E-mail: glingwang@cmu.edu.cn

[c] State Key Laboratory of Fine Chemicals, Dalian University of Technology, Dalian, China. E-mail: dujj@dlut.edu.cn

† These authors contributed equally to this work.

1 Experimental section

General

Unless otherwise stated, all chemical substances and organic solvents used were analytical grade and obtained from Energy Chemical & Technology (Shanghai) Co. Ltd. without extra purification. A VARIAN Mercury 500 MHz spectrometer was employed to record ^{1}H NMR spectra. Chemical shifts in ^{1}H NMR (δ) are presented in ppm downfield from Me_4Si, as estimated by residual chloroform (δ 7.26 ppm). On a VARIAN Mercury 125 MHz spectrometer, ^{13}C NMR spectra were recorded in $CDCl_3$, reported in ppm with the internal chloroform signal at δ=77.0 ppm as the reference. The precise molecular weight of the product is determined utilizing a high resolution mass spectrometer. A UV-2550 spectrophotometer was used to record an absorption spectroscopy at 298 K. Fluorescence spectra are presented as cm^{-1} and were captured using an F-128 spectrophotometer. Laser particle size analyzer was bought from Malvern. The temperature of the solution is tracked by a temperature determining camera. The light source employed for light irradiation was a 808 nm laser that was purchased from Changchun New Industries Optoelectronics Technology and controlled by a fiber linked laser system for the laser output power. A CEL-NP 2000 power meter was implemented for evaluating the optical power density which was obtained from Beijing Zhong Jiao Jin Yuan Technology Co, Ltd. In the CCK8 assessment, a BioTek Synergy H1 microplate reader was utilized. Fluorescence imaging was estimated using an Olympus Confocal Laser Fluorescence Microscope FV1200 (Japan). The flow cytometric analysis was used the BD FACSVerse™ Flow Cytometer.

Singlet Oxygen Detection

Utilizing 1,3-diphenylisobenzofuran (DPBF), the $^{1}O_2$ production in toluene was determined.[1-3] The absorbance of DPBF at 416 nm was adjusted to about 1.4 in toluene and the absorbance of dye molecule was adjusted to about 0.8. The characteristic absorption of DPBF was applied to characterize $^{1}O_2$ production. The absorption value of the dye molecule indicates the photo-stability of the dye. The

808 nm laser light source is used, the optical radiation power is 0.1 W/cm^2, and the illuminated time is 0-30 min.

The Preparation of dye-nanoparticles

Nano-deposition method was used for preparation.[4-7] 1 ml THF solution containing 1 mg dye and 5 mg DSPE-PEG$_{2000}$ is slowly but steadily injected to the 10 ml aqueous solution. Following that, THF was volatilized by constant stirring for 24 h to ensure that dye was evenly spread in the solution. By centrifuging the appropriate NPs at 6000 rpm for 5 min, the final produces could be attained.

Photothermal effect and efficiency

A variety of concentrations were created (0-80 μM), and all of them were exposed to 0.8 W/cm^2 of an 808 nm laser for 5 min. The temperature was measured every 30 s using an infrared thermal imaging camera. Meanwhile, 30 μM dye was treated by 808 nm laser at various power densities (0.2-0.8 W/cm^2) for 5 min. The temperature was collected by the infrared thermal imaging camera every 30 s. The solution was cooled following 5 min of light irradiation. During this process, the solution temperature was monitored every 30 s. The photothermal conversion efficiencies (η) was calculated using the following method.[8-10]

$$\eta = \frac{hs(T_{Max} - T_{Surr}) - Q_{Dis}}{I(1 - 10^{-A})}$$

h means heat transfer coefficient, *s* was for container surface area, Q_{Dis} stands for heat dispersed from the laser via the solvent and container, *I* was for laser power, and *A* represents for absorbance at excitation wavelength. η denotes photothermal conversion efficiency.

$$hs = \frac{mC}{\tau_s}$$

m is the total quantity of the photothermal reagent containing solution, *C* represents the temperature coefficient, and τ_s is the relevant time constant.

$$t = -\tau_s ln(\theta)$$

The temperature of the driving force is a non-dimensional parameter termed θ.

$$\theta = \frac{T - T_{Surr}}{T_{Max} - T_{Surr}}$$

T is the current temperature, T_{Max} is the highest steady state temperature, and T_{surr} denotes the surrounding temperature.

Cytotoxicity assay by CCK8 testing

For the dark cytotoxicity investigation, SW620 cells treated with NPs (0-40 μM) in DMEM medium for 4 h but without laser irradiation were also used. For photo-cytotoxicity assessment, various concentrations of NPs (0-40 μM) in DMEM medium were added to the wells respectively for 4 h. The cells were then subjected to 808 nm laser irradiation (0.3 W/cm^2) for 20 min. 100 μL of MTT solution (0.5 mg ml^{-1}) in DMEM was added to each well after a further 24 h of incubation, and the cells were then incubated at 37 °C for an additional 4 h. After cautiously sucking off the medium, each well was given 100 μL of DMSO to dissolve the formazan crystals that had formed, and a microplate reader was used to determine the absorbance at 490 nm.[11-12] The following equation was used to determine the cell viability:

Cell viability (%) = (OD_{dye} − OD_{blank}/$OD_{control}$ − OD_{blank}) × 100%

Dead/Live Cell Co-Staining Fluorescence Imaging

4T1 cells were planted into confocal dishes, cultured for 24 h, and then divided into the four groups: the control group, the light group, the dye-NPs group, and the dye-NPs plus light group. After 2 h, cells were stained with calcein AM and PI double-staining kits and took pictures using confocal laser scanning microscopy.[13-14] The concentration of dye-NPs is 30 μM. A 20 min exposure was performed using a 0.3 W/cm^2 NIR laser at 808 nm. Excited was set at 488 nm, detected at 500-550 nm for calcein AM channel and 600-700 nm for PI channel.

Flow cytometry experiments

The group of cells and the setting of dye-NPs concentration and light intensity were referred to the double-staining experiment. Using the Annexin V-FITC/propidium iodide (PI) Apoptosis Detection Kit, cells were digested and dispersed into Bind Buffer to produce a single cell suspension after 2 h of treatment. [15-16] The treated cells were collected via trypsinization, and the Annexin V-FITC apoptosis detection kit was utilized to determine the extent of apoptosis (Beyotime Biotechnology).

Synthesis

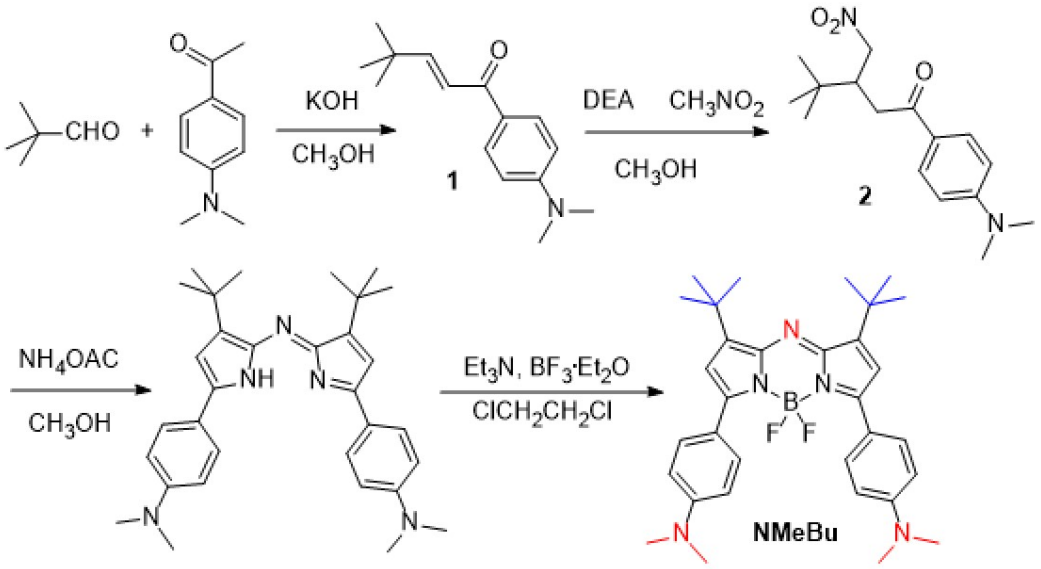

Synthesis of (E)-1-(4-(dimethylamino)phenyl)-4,4-dimethylpent-2-en-1-one **1**

pivalaldehyde (2 ml, 18.4 mmol) was added to 1-(4-(dimethylamino)phenyl)ethan-1-one (3 g, 18.4 mmol) in 30 ml methanol. Then 4 g KOH in 2 ml H_2O was added to the mixture, and this mixture was refluxed for 24 h. After cooling to room temperature, the mixture was extracted with CH_2Cl_2 (2 × 50 ml), and the organic layer was washed with brine (2 × 50 ml) and dried over anhydrous Na_2SO_4. The solvents were removed by evaporation, and the resulting crude mixture was separated by column chromatography (CH_2Cl_2/*n*-hexane =1:3) to

afford light yellow solids as compound **1** (3.49 g, 15.1 mmol, 82%). ^{1}H NMR (400 MHz, $CDCl_3$): δ (ppm) 7.91 (d, ^{3}J = 9.2 Hz, 2H), 7.01 (d, ^{3}J = 15.6 Hz, 1H), 6.82 (d, ^{3}J = 15.6 Hz, 1H), 6.67 (d, ^{3}J = 9.2 Hz, 2H), 3.05 (s, 6H), 1.14 (s, 9H). ^{13}C NMR (125 MHz, $CDCl_3$): 189.1, 157.0, 153.3, 130.8, 126.1, 120.6, 110.8, 40.1, 34.0, 29.0.

Synthesis of 1-(4-(dimethylamino)phenyl)-4,4-dimethyl-3-(nitromethyl)pentan-1-one **2**

Diethylamine (9 ml) and nitromethane (8 ml) were added to compound **1** (3.49 g, 15.1 mmol) in anhydrous methanol (40 ml). The mixture was refluxed for 72 h. After cooling to room temperature, the mixture was extracted with CH_2Cl_2 (2 × 50 ml), and the organic layer was washed with brine (2 × 50 ml) and dried over anhydrous Na_2SO_4. The solvent was removed under reduced pressure, and resulting crude mixture was separated by column chromatography (CH_2Cl_2:*n*-hexane = 3:2) to afford compound **2** (1.81 g, 6.19 mmol, 41%) as orange solid powder. ^{1}H NMR (400 MHz, $CDCl_3$): δ (ppm) 7.87 (d, ^{3}J = 9.2 Hz, 2H), 6.65 (d, ^{3}J = 9.2 Hz, 2H), 4.54 (dd, ^{2}J = 12.8 Hz, ^{3}J = 6.8 Hz, 1H), 4.39 (dd, ^{2}J = 12.8 Hz, ^{3}J = 6.8 Hz, 1H), 3.15 (dd, ^{2}J = 16.0 Hz, ^{4}J = 3.6 Hz, 1H), 3.05 (s, 6H), 2.92-2.99 (m, 1H), 2.87 (dd, ^{2}J = 16.0 Hz, ^{3}J = 8.0 Hz, 1H), 0.97 (s, 9H). ^{13}C NMR (125 MHz, $CDCl_3$): 196.1, 153.6, 130.3, 124.7, 110.7, 42.4, 40.1, 36.3, 33.4, 29.7, 27.5.

Synthesis of dye **NMeBu**

NH_4OAc (15 g, 194.5 mmol) was added to compound **2** (1.81 g, 6.19 mmol) in anhydrous methanol (30 ml). The mixture was refluxed for 24 h. After cooling to room temperature, the mixture was extracted with CH_2Cl_2 (2 × 50 ml), and the organic layer was washed with brine (2 × 50 ml) and dried over anhydrous Na_2SO_4. After the solvent was removed under reduced pressure, and resulting crude mixture was separated by column chromatography (CH_2Cl_2: *n*-hexane =1:2) to afford the precursor (1.56 g, 3.15 mmol) as dark green solid powder. This precursor was dissolved in 30 ml anhydrous $ClCH_2CH_2Cl$. Triethylamine (0.5 ml, 3.6 mmol) was

added and stirred at room temperature for 30 min, followed by dropwise addition of $BF_3 \cdot Et_2O$ (1 ml, 7.9 mmol) with stirring at room temperature for 30 min. The mixture was then heated in 75 ℃ for 2 h. After cooling to room temperature, the mixture was extracted with CH_2Cl_2 (2 × 50 ml), and the organic layer was washed with brine (2 × 50 ml) and dried over anhydrous Na_2SO_4. After solvent removal by evaporation, and the resulting crude product was separated by column chromatography (CH_2Cl_2/*n*-hexane = 2:3) to afford dye **NMeBu** (0.667 g, 1.23 mmol, 19%) as yellowish brown solid powder with metallic luster. ^{1}H NMR (400 MHz, $CDCl_3$): δ (ppm) 8.02 (d, ^3J = 8.8 Hz, 4H), 6.73 (d, ^3J = 8.8 Hz, 4H), 6.60 (s, 2H), 3.05 (s, 12H), 1.47 (s, 18H). ^{13}C NMR (125 MHz, $CDCl_3$): 155.4, 153.8, 151.6, 143.3, 131.5, 119.6, 118.0, 111.8, 40.2, 33.1, 31.1. HRMS (ESI) m/z calcd for $C_{32}H_{40}BF_2N_5Na^+$ $(M+Na)^+$ 566.32370, found 566.32172.

2 Figures and Tables

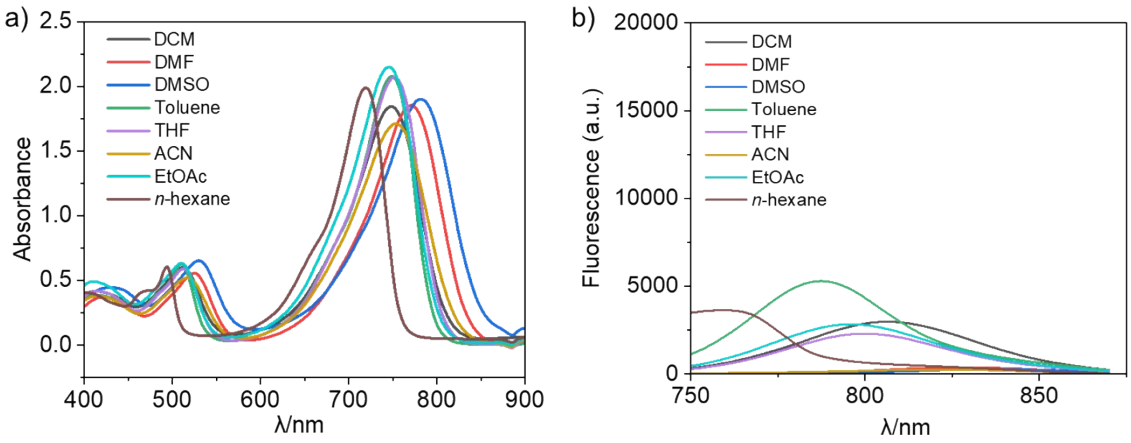

Fig. S1 a) Absorption spectra of **NMeBu** in different solvents; b) Emission spectra of **NMeBu** in different solvents. Solvents included DCM, DMF, DMSO, Toluene, THF, ACN, EtOAc and *n*-hexane.

Table S1 Spectroscopic properties of **NMeBu** in various solvents at 298 K.

Solvents	λ_{abs} [nm]/ λ_{em} [nm]	Stokes shift (nm)	FWHM (nm)	ε [M^{-1} cm^{-1}]
DCM	748/805	57	87.63	86000
DMF	772/828	56	91.98	85500
DMSO	782/837	55	96.15	85000
Toluene	750/787	37	73.66	86500
THF	752/800	48	81.75	86300
ACN	752/819	67	95.87	86300
EtOAc	746/796	50	85.32	85000
n-hexane	720/758	38	62.40	86100

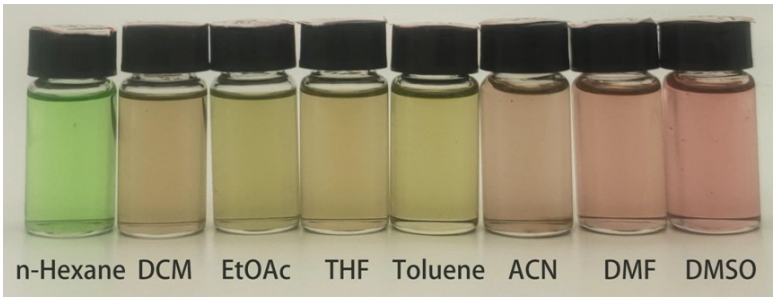

Fig. S2 The colors of dye **NMeBu** in different solvents under sunlight.

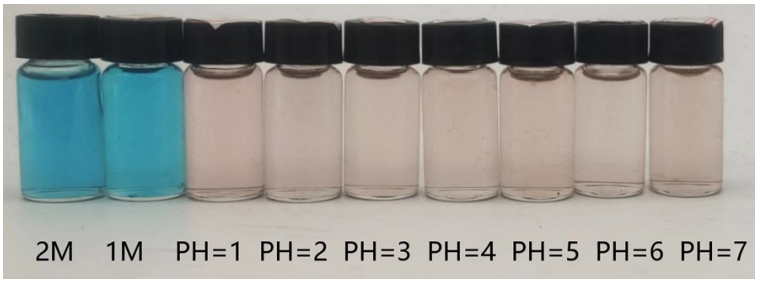

Fig. S3 The colors of dye **NMeBu** in different pH=7-1 and 1-2 M HCl under sunlight.

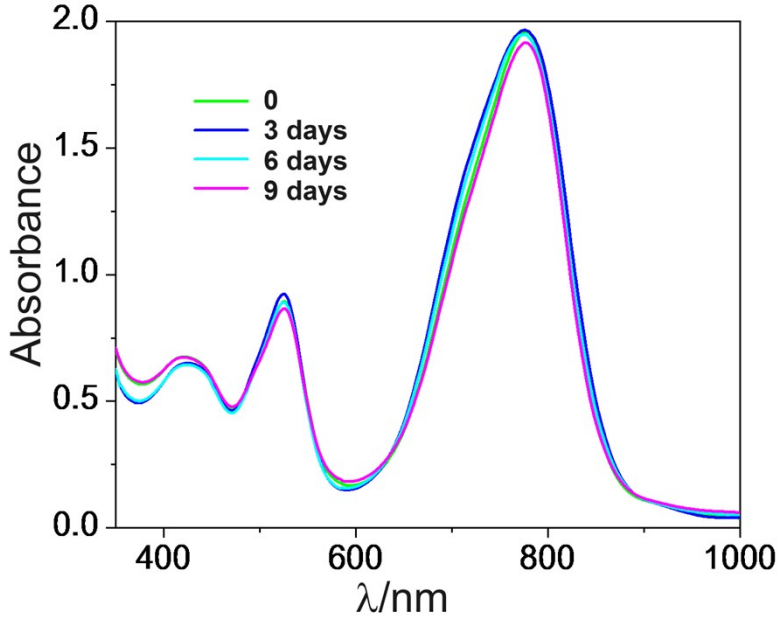

Fig. S4 Absorption Intensities of **NMeBu**-NPs in the aqueous solution for 0, 3, 6 and 9 days at room temperature.

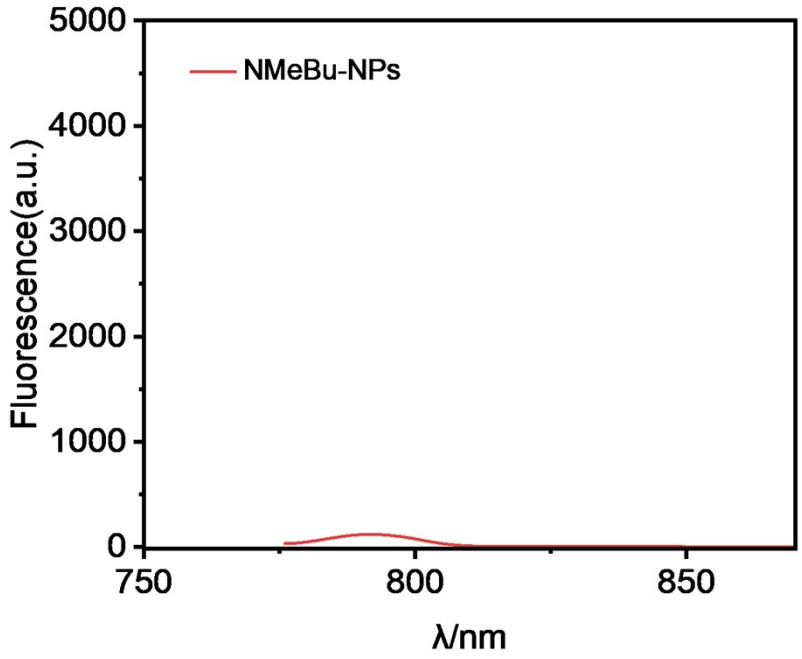

Fig. S5 Fluorescence spectrum of **NMeBu**-NPs in aqueous solution.

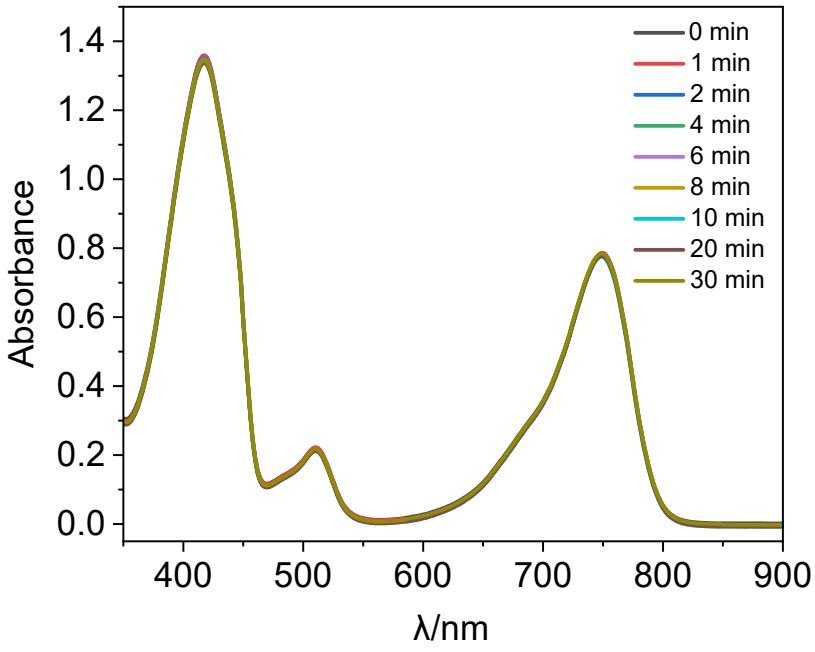

Fig. S6 Absorption spectra of DPBF and dye **NMeBu** under 30 min irradiation in toluene solution.

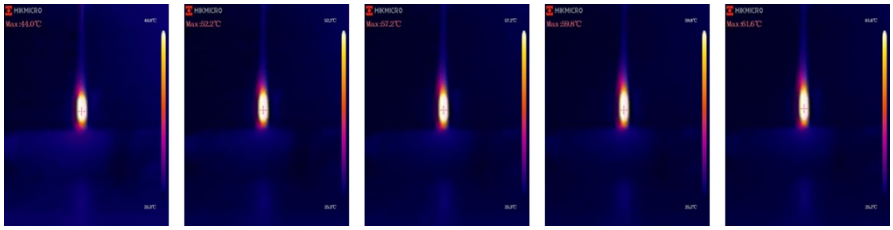

Fig. S7 Infrared thermal images of 80 μM **NMeBu**-NPs under laser irradiation (808 nm, 0.8 W/cm^2) for 1, 2, 3, 4, 5 min.

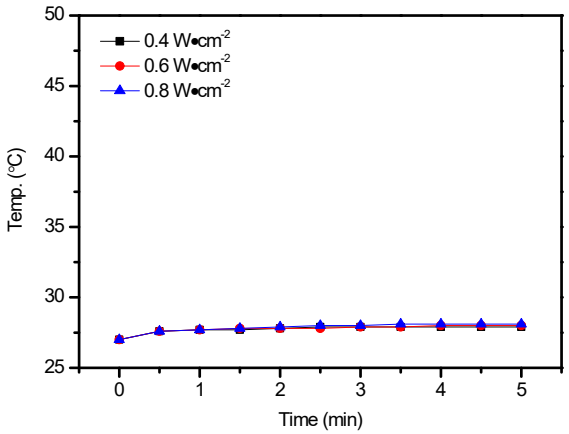

Fig. S8 Temperature of pure aqueous solution under various power density (0.4, 0.6, 0.8 W/cm^2) radiation within 5 min.

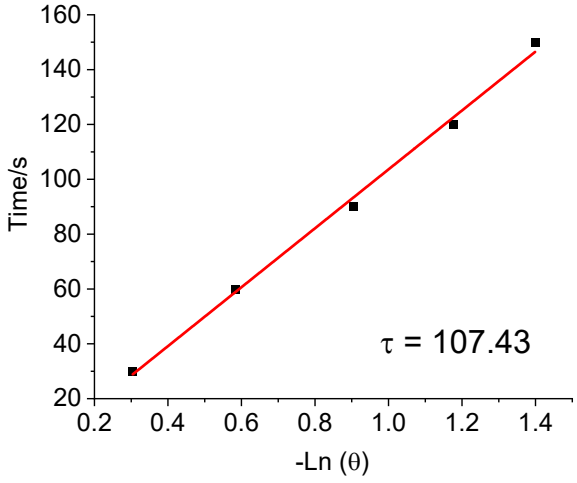

Fig. S9 The system time constant for **NMeBu** heat transfer was determined by plotting linear time data from the cooling phase of the system against the negative natural logarithm of the temperature of the system driving force.

3 NMR and HRMS

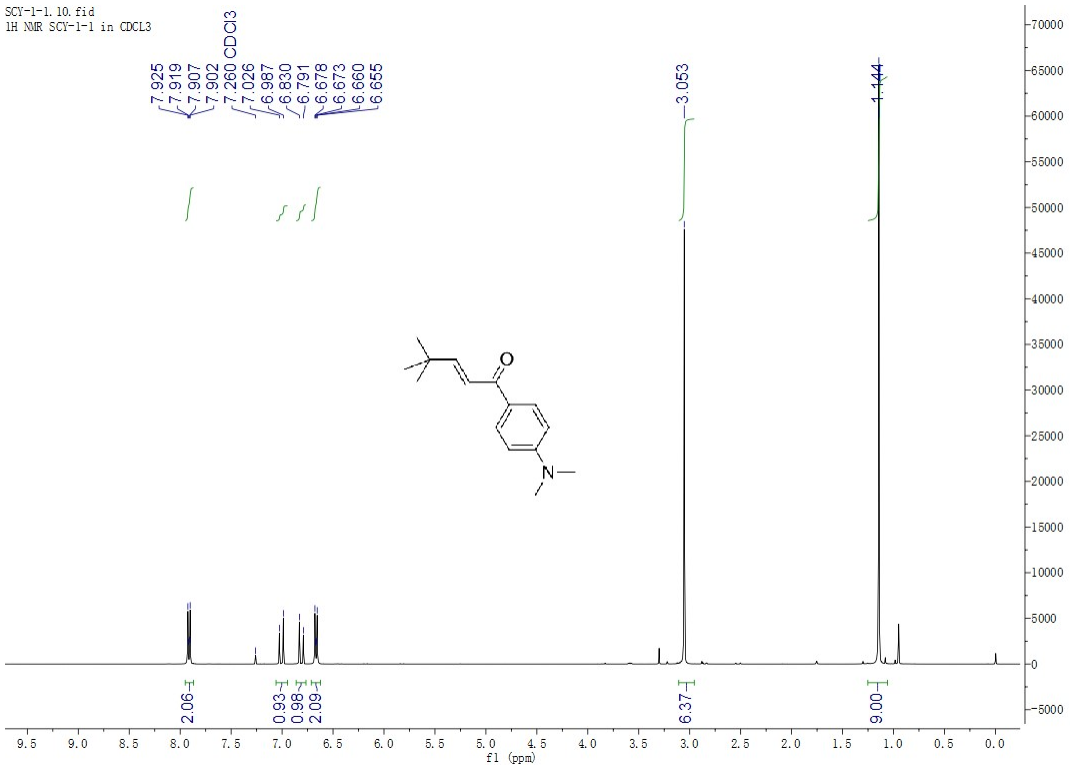

^{1}H NMR of **1**

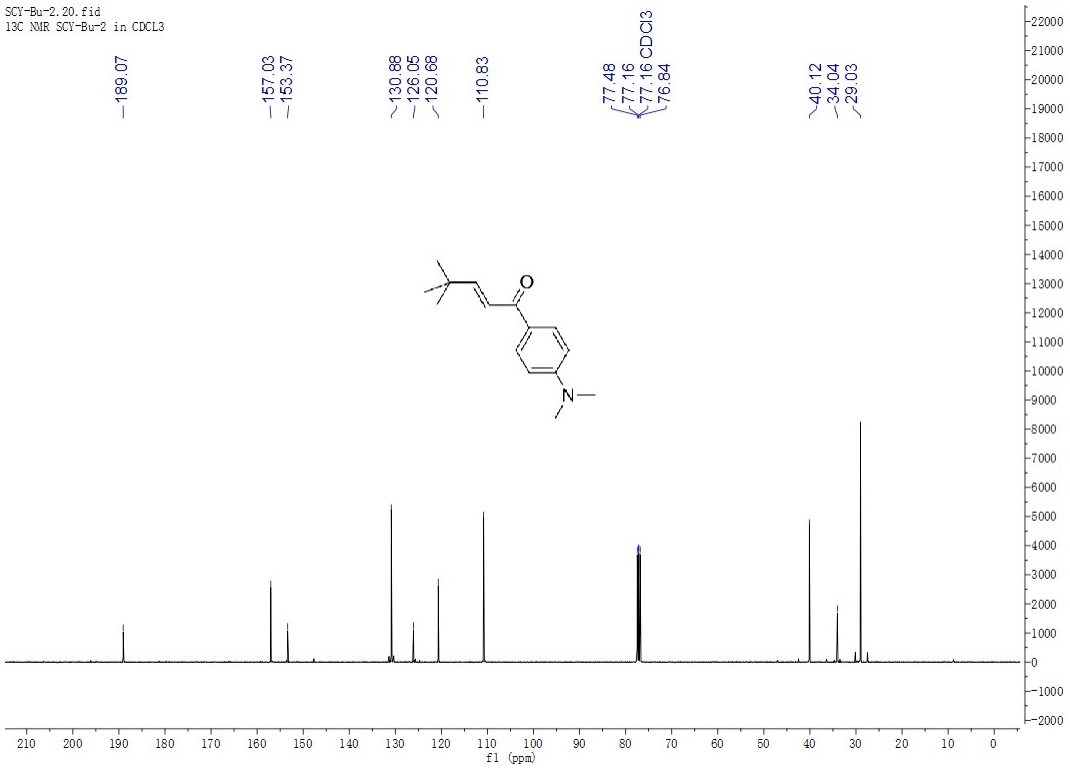

^{13}C NMR of **1**

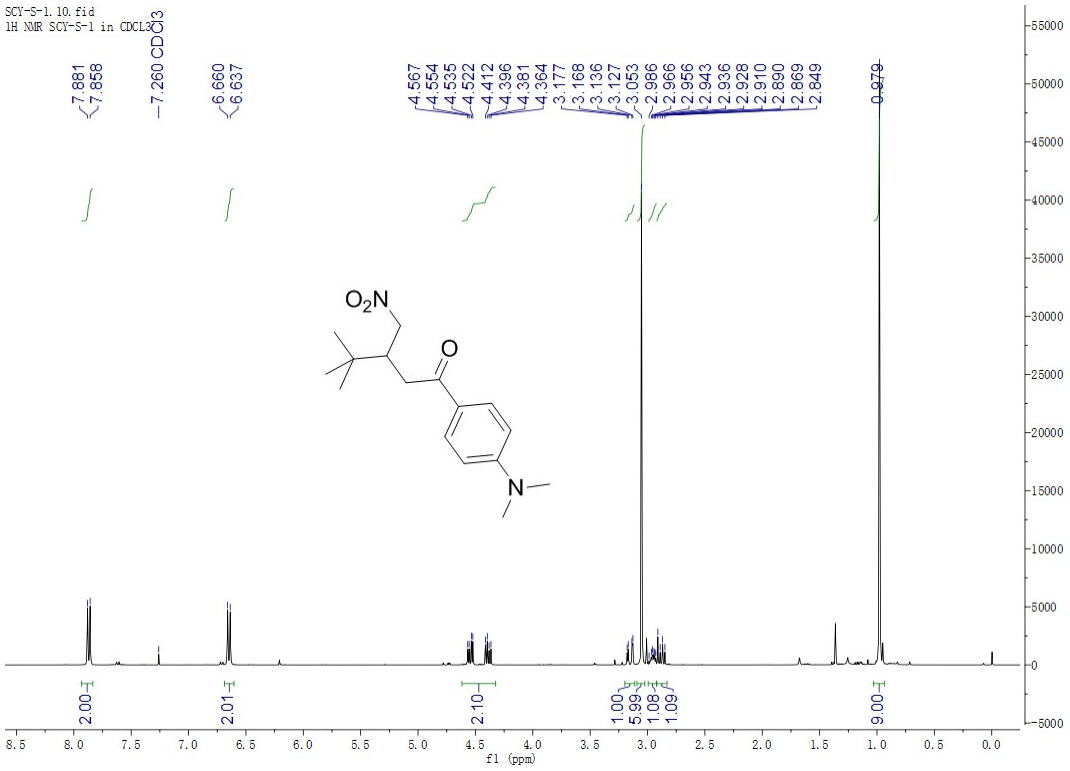

^{1}H NMR of **2**

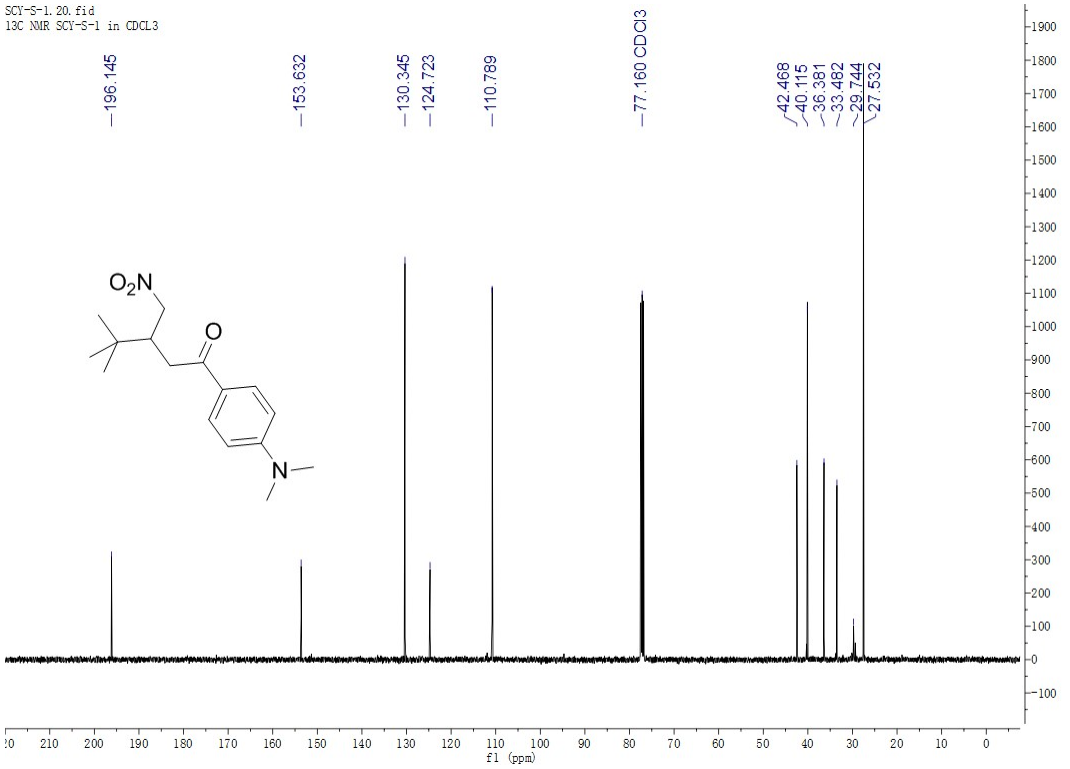

^{13}C NMR of **2**

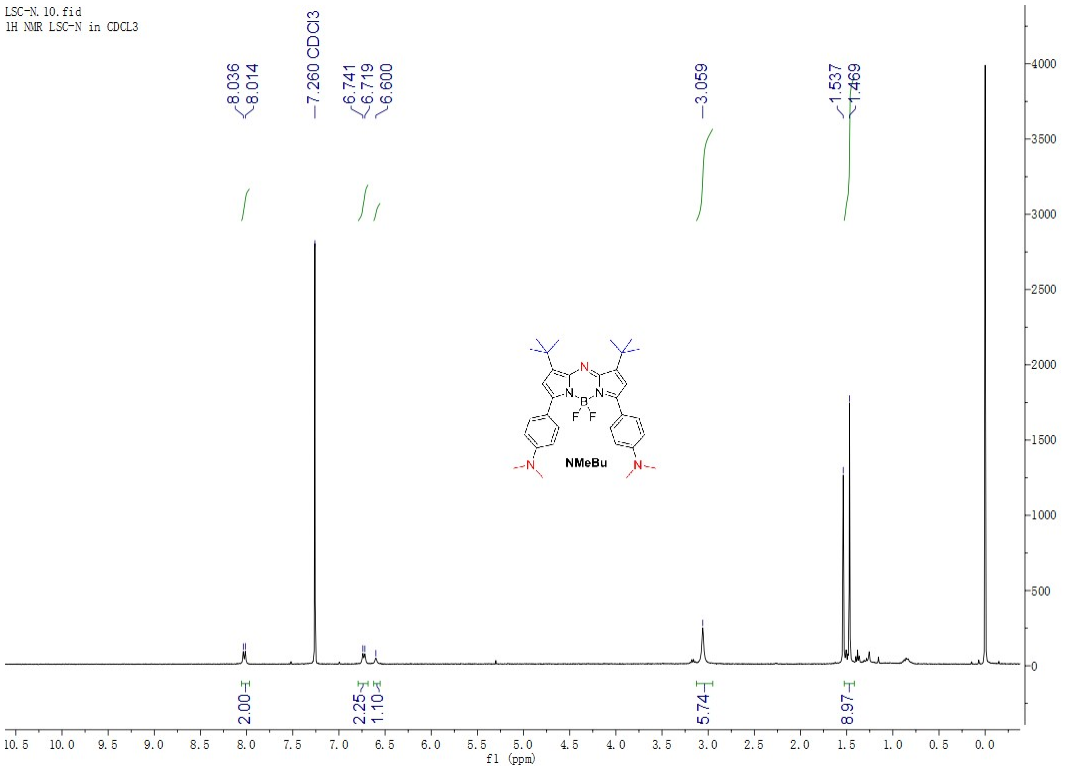

^{1}H NMR of **NMeBu**

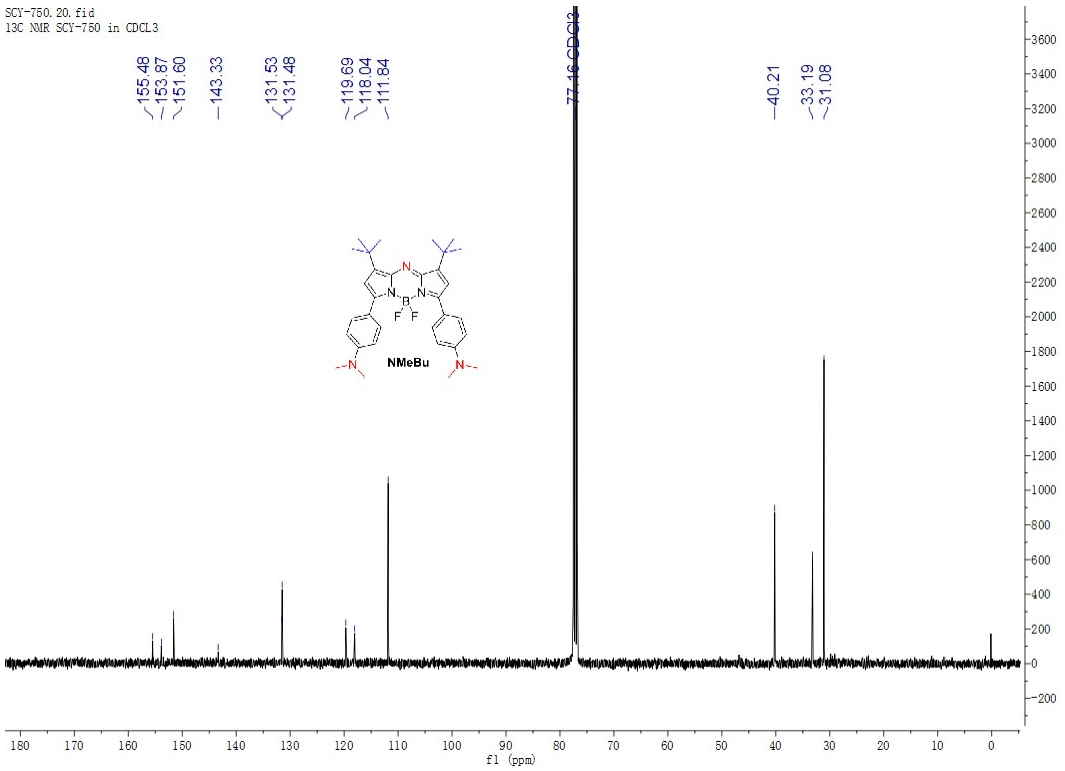

^{13}C NMR of **NMeBu**

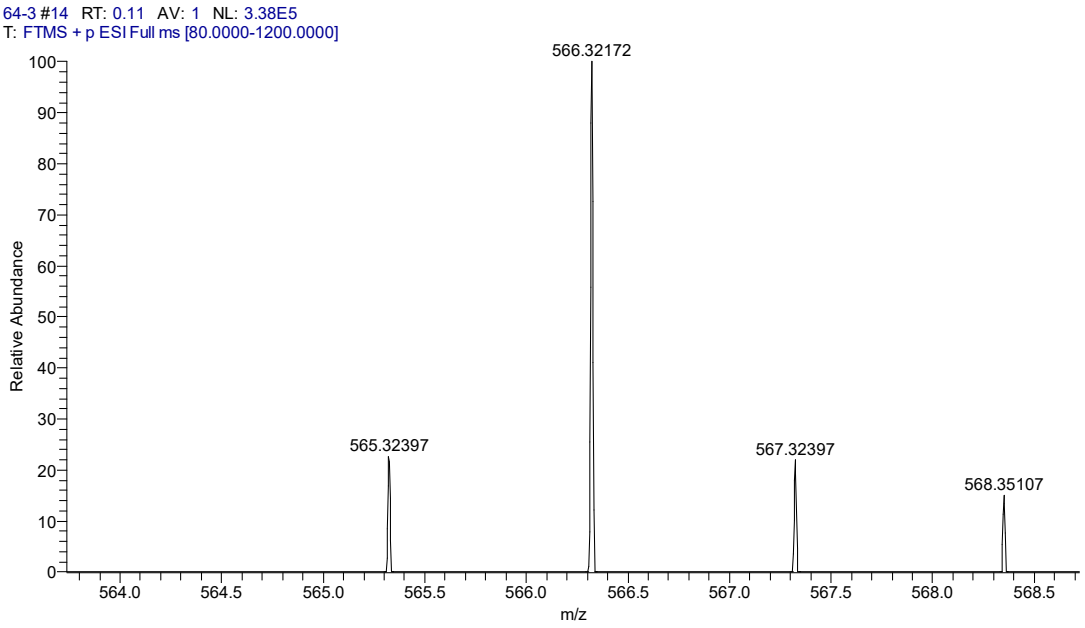

NMeBu: HRMS (ESI) m/z calcd for $C_{32}H_{40}BF_2N_5Na^+$ $(M+Na)^+$ 566.32370,found 566.32172.

4 X-ray data of NMeBu

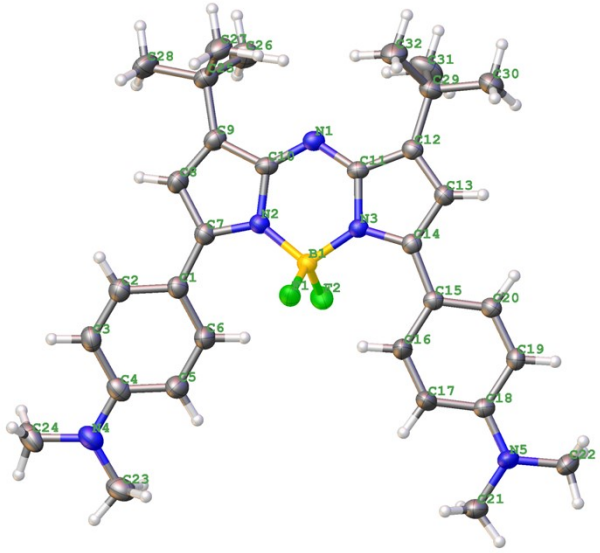

Table 1 Crystal data and structure refinement for tbu-scy.

Identification code	tbu-scy
Empirical formula	$C_{32}H_{40}BF_2N_5$
Formula weight	543.50
Temperature/K	169.99(10)
Crystal system	monoclinic
Space group	$P2_1/c$
a/Å	22.9511(8)
b/Å	11.1234(4)
c/Å	11.6931(4)
α/°	90
β/°	91.289(3)
γ/°	90
Volume/Å^3	2984.43(18)
Z	4
ρ_{calc}g/cm^3	1.210
μ/mm^{-1}	0.644
F(000)	1160.0
Crystal size/mm^3	0.15 × 0.13 × 0.11
Radiation	Cu Kα (λ = 1.54184)
2Θ range for data collection/°	7.706 to 147.668
Index ranges	-28 ≤ h ≤ 27, -13 ≤ k ≤ 7, -14 ≤ l ≤ 13
Reflections collected	11311
Independent reflections	5849 [R_{int} = 0.0428, R_{sigma} = 0.0648]
Data/restraints/parameters	5849/0/371
Goodness-of-fit on F^2	0.995

Final R indexes [I>=2σ (I)] $R_1 = 0.0523$, $wR_2 = 0.1269$

Final R indexes [all data] $R_1 = 0.0785$, $wR_2 = 0.1468$

Largest diff. peak/hole / e Å^{-3} 0.20/-0.21

Crystal structure determination of [tbu-scy]

Crystal Data for $C_{32}H_{40}BF_2N_5$ (M =543.50 g/mol): monoclinic, space group $P2_1/c$ (no. 14), a = 22.9511(8) Å, b = 11.1234(4) Å, c = 11.6931(4) Å, β = 91.289(3)°, V = 2984.43(18) Å^3, Z = 4, T = 169.99(10) K, μ(Cu Kα) = 0.644 mm^{-1}, $Dcalc$ = 1.210 g/cm^3, 11311 reflections measured (7.706° ≤ 2Θ ≤ 147.668°), 5849 unique (R_{int} = 0.0428, R_{sigma} = 0.0648) which were used in all calculations. The final R_1 was 0.0523 (I >2σ(I)) and wR_2 was 0.1468 (all data).

Table 2 Fractional Atomic Coordinates (×10^4) and Equivalent Isotropic Displacement Parameters (Å^2×10^3) for tbu-scy. U_{eq} is defined as 1/3 of the trace of the orthogonalised U_{IJ} tensor.

Atom	*x*	*y*	*z*	U(eq)
F1	3175.6(5)	5583.6(10)	3242.8(10)	31.4(3)
F2	2906.5(5)	3665.0(10)	3667.9(10)	35.3(3)
N1	1626.9(7)	5029.1(15)	1804.4(14)	28.1(4)
N2	2167.9(7)	5224.0(15)	3589.2(14)	27.0(4)
N3	2631.5(7)	4408.9(14)	1829.3(13)	25.3(3)
N4	3460.1(9)	6031.3(18)	8678.6(16)	43.7(5)
N5	5284.7(8)	1977.9(18)	1645.8(16)	39.6(5)
C1	2433.6(9)	5783.3(19)	5639.1(17)	31.5(4)
C2	2308.0(10)	6614.9(19)	6506.8(18)	34.7(5)
C3	2640.0(10)	6709(2)	7495.1(18)	37.0(5)
C4	3130.4(10)	5960(2)	7692.9(18)	36.2(5)
C5	3264.6(10)	5139(2)	6824.1(19)	41.6(5)
C6	2925.4(10)	5058(2)	5839.6(19)	40.2(5)
C7	2048.2(9)	5706.9(18)	4641.1(17)	30.0(4)
C8	1461.9(9)	6129(2)	4603.3(18)	34.2(5)
C9	1216.7(9)	5910.4(19)	3543.3(18)	31.3(4)
C10	1665.7(8)	5355.3(18)	2896.4(17)	28.6(4)
C11	2084.0(8)	4565.2(17)	1293.1(17)	26.6(4)
C12	2103.3(9)	4101.0(18)	153.2(17)	28.7(4)
C13	2655.4(9)	3667.0(18)	33.5(17)	29.7(4)
C14	2979.4(8)	3829.5(17)	1073.2(16)	26.6(4)
C15	3576.1(8)	3402.9(17)	1269.6(16)	26.9(4)

Table 2 Fractional Atomic Coordinates ($\times 10^4$) and Equivalent Isotropic Displacement Parameters ($Å^2 \times 10^3$) for tbu-scy. U_{eq} is defined as 1/3 of the trace of the orthogonalised U_{IJ} tensor.

Atom	*x*	*y*	*z*	U(eq)
C16	3942.7(10)	3688(2)	2200(2)	42.8(6)
C17	4497.3(10)	3230(2)	2321(2)	46.8(6)
C18	4730.3(9)	2434(2)	1524.4(17)	31.5(4)
C19	4367.4(9)	2154.6(19)	580.8(18)	33.3(5)
C20	3815.5(9)	2627.9(18)	462.3(18)	30.9(4)
C21	5592.5(10)	2043(2)	2743.9(19)	43.9(6)
C22	5504.5(10)	1168(2)	800(2)	45.3(6)
C23	3969.9(11)	5276(2)	8839(2)	50.0(6)
C24	3245.9(12)	6690(2)	9665(2)	48.8(6)
C25	599.6(9)	6158(2)	3122.7(19)	37.1(5)
C26	306.7(10)	4965(2)	2771(2)	51.6(7)
C27	609.4(10)	7015(2)	2090(2)	45.4(6)
C28	249.6(10)	6749(3)	4069(2)	50.8(7)
C29	1595.2(9)	4026(2)	-698.9(18)	35.2(5)
C30	1801.6(11)	3562(2)	-1855(2)	47.4(6)
C31	1140.8(12)	3163(3)	-229(2)	58.3(7)
C32	1324.3(11)	5278(2)	-879(2)	48.6(6)
B1	2738.2(10)	4718.6(19)	3105.5(19)	25.0(4)

Table 3 Anisotropic Displacement Parameters ($Å^2 \times 10^3$) for tbu-scy. The Anisotropic displacement factor exponent takes the form: $-2\pi^2[h^2a^{*2}U_{11}+2hka^*b^*U_{12}+\ldots]$.

Atom	U_{11}	U_{22}	U_{33}	U_{23}	U_{13}	U_{12}
F1	25.5(6)	33.5(6)	35.2(6)	-7.2(5)	0.2(5)	-4.3(5)
F2	46.0(7)	28.6(6)	31.1(6)	2.1(5)	-5.7(5)	7.0(5)
N1	23.8(9)	32.1(8)	28.5(9)	1.1(7)	0.2(7)	-0.7(7)
N2	25.1(9)	31.4(8)	24.3(8)	-1.0(7)	-0.6(6)	0.8(7)
N3	21.9(8)	27.7(8)	26.1(8)	-1.3(6)	-0.3(6)	1.0(6)
N4	47.4(12)	50.6(11)	32.9(10)	-4.6(9)	-7.6(8)	0.2(10)
N5	27.9(10)	53.7(11)	36.9(10)	-11.6(9)	-6.9(7)	13.4(9)
C1	29.9(11)	38.3(11)	26.5(10)	-2.1(9)	2.6(8)	-0.2(9)
C2	33.0(12)	36.9(11)	34.2(11)	-3.2(9)	2.7(9)	1.3(9)
C3	41.3(13)	37.8(11)	32.0(11)	-7.6(9)	2.6(9)	-0.2(10)
C4	37.1(12)	43.7(12)	27.9(10)	-0.4(9)	-0.3(9)	-7.0(10)
C5	38.5(13)	54.5(14)	31.8(11)	-3.1(11)	-1.5(9)	10.0(11)
C6	37.3(12)	52.3(13)	30.9(11)	-7.9(10)	-0.3(9)	9.4(11)

Table 3 Anisotropic Displacement Parameters ($Å^2×10^3$) for tbu-scy. The Anisotropic displacement factor exponent takes the form: $-2\pi^2[h^2a^{*2}U_{11}+2hka^*b^*U_{12}+\ldots]$.

Atom	U_{11}	U_{22}	U_{33}	U_{23}	U_{13}	U_{12}
C7	28.0(11)	33.7(10)	28.6(10)	-1.1(8)	3.5(8)	-0.1(8)
C8	26.7(11)	42.1(11)	34.0(11)	-5.4(9)	5.3(8)	1.4(9)
C9	23.9(10)	35.6(10)	34.6(11)	0.7(9)	4.3(8)	0.9(8)
C10	21.1(10)	32.8(10)	31.7(10)	1.8(8)	-1.9(8)	-0.3(8)
C11	21.2(10)	28.5(9)	29.8(10)	2.0(8)	-2.3(7)	0.2(8)
C12	27.0(10)	28.7(9)	30.2(10)	-1.7(8)	-2.3(8)	-0.7(8)
C13	27.4(11)	33.2(10)	28.3(10)	-3.7(8)	-0.8(8)	1.5(8)
C14	26.4(10)	26.0(9)	27.3(10)	-1.2(8)	0.4(8)	-0.3(8)
C15	24.1(10)	28.3(9)	28.2(10)	-0.8(8)	-0.9(7)	0.8(8)
C16	30.3(12)	59.3(15)	38.5(12)	-21.1(11)	-5.5(9)	11.2(11)
C17	32.7(12)	69.1(16)	38.0(13)	-22.6(12)	-11.5(10)	13.3(12)
C18	26.3(11)	37.3(10)	30.7(11)	-3.2(9)	-2.6(8)	4.0(9)
C19	34.3(12)	33.4(10)	32.2(11)	-8.8(9)	-1.5(8)	6.4(9)
C20	29.3(11)	31.0(10)	32.2(11)	-5.2(8)	-5.3(8)	2.2(8)
C21	33.0(12)	60.0(15)	38.3(13)	-7.5(11)	-9.1(10)	12.7(11)
C22	36.3(13)	58.3(15)	41.0(13)	-10.9(11)	-5.0(10)	19.5(11)
C23	52.6(16)	57.0(15)	39.7(13)	2.5(12)	-13.7(11)	2.4(13)
C24	70.9(18)	42.1(12)	33.0(12)	-6.0(11)	-10.7(11)	-2.0(12)
C25	24.0(11)	46.1(12)	41.1(12)	-2.5(10)	1.1(9)	2.8(9)
C26	29.2(13)	59.3(16)	66.2(18)	-7.0(13)	0.7(11)	-8.4(11)
C27	36.8(13)	53.5(14)	45.9(14)	2.8(11)	-1.7(10)	13.6(11)
C28	28.3(12)	76.4(18)	48.0(14)	-6.7(14)	5.7(10)	12.1(12)
C29	28.8(11)	44.2(12)	32.3(11)	-4.4(10)	-6.5(8)	1.3(9)
C30	41.1(14)	62.4(16)	38.1(13)	-12.2(12)	-11.7(10)	7.4(12)
C31	46.0(15)	75.4(19)	52.9(16)	-2.5(15)	-10.4(12)	-24.8(14)
C32	42.9(14)	60.0(15)	42.4(13)	-1.6(12)	-10.2(11)	15.7(12)
B1	25.3(11)	23.5(10)	26.0(11)	0.3(9)	-1.3(8)	0.1(8)

Table 4 Bond Lengths for tbu-scy.

Atom	Atom	Length/Å	Atom	Atom	Length/Å
F1	B1	1.397(2)	C5	C6	1.378(3)
F2	B1	1.394(2)	C7	C8	1.425(3)
N1	C10	1.328(3)	C8	C9	1.371(3)
N1	C11	1.324(3)	C9	C10	1.432(3)
N2	C7	1.376(2)	C9	C25	1.514(3)

Table 4 Bond Lengths for tbu-scy.

Atom	Atom	Length/Å	Atom	Atom	Length/Å
N2	C10	1.401(2)	C11	C12	1.431(3)
N2	B1	1.543(3)	C12	C13	1.366(3)
N3	C11	1.403(2)	C12	C29	1.519(3)
N3	C14	1.366(2)	C13	C14	1.422(3)
N3	B1	1.546(3)	C14	C15	1.463(3)
N4	C4	1.367(3)	C15	C16	1.396(3)
N4	C23	1.449(3)	C15	C20	1.400(3)
N4	C24	1.462(3)	C16	C17	1.375(3)
N5	C18	1.374(3)	C17	C18	1.400(3)
N5	C21	1.453(3)	C18	C19	1.402(3)
N5	C22	1.437(3)	C19	C20	1.376(3)
C1	C2	1.408(3)	C25	C26	1.540(3)
C1	C6	1.403(3)	C25	C27	1.539(3)
C1	C7	1.451(3)	C25	C28	1.530(3)
C2	C3	1.374(3)	C29	C30	1.532(3)
C3	C4	1.415(3)	C29	C31	1.529(3)
C4	C5	1.406(3)	C29	C32	1.538(3)

Table 5 Bond Angles for tbu-scy.

Atom	Atom	Atom	Angle/°	Atom	Atom	Atom	Angle/°
C11	N1	C10	120.25(17)	C11	C12	C29	126.26(18)
C7	N2	C10	107.34(16)	C13	C12	C11	105.73(17)
C7	N2	B1	131.15(17)	C13	C12	C29	127.85(19)
C10	N2	B1	121.28(16)	C12	C13	C14	109.62(18)
C11	N3	B1	121.66(16)	N3	C14	C13	108.13(17)
C14	N3	C11	107.46(16)	N3	C14	C15	127.61(17)
C14	N3	B1	130.37(16)	C13	C14	C15	124.24(17)
C4	N4	C23	120.4(2)	C16	C15	C14	126.46(18)
C4	N4	C24	120.3(2)	C16	C15	C20	115.23(18)
C23	N4	C24	118.24(19)	C20	C15	C14	118.31(17)
C18	N5	C21	120.22(18)	C17	C16	C15	122.4(2)
C18	N5	C22	119.92(18)	C16	C17	C18	122.2(2)
C22	N5	C21	117.91(18)	N5	C18	C17	122.10(19)
C2	C1	C7	119.16(19)	N5	C18	C19	122.12(19)
C6	C1	C2	115.8(2)	C17	C18	C19	115.76(19)
C6	C1	C7	125.05(19)	C20	C19	C18	121.58(19)

Table 5 Bond Angles for tbu-scy.

Atom	Atom	Atom	Angle/°	Atom	Atom	Atom	Angle/°
C3	C2	C1	122.5(2)	C19	C20	C15	122.83(19)
C2	C3	C4	121.1(2)	C9	C25	C26	109.25(19)
N4	C4	C3	121.8(2)	C9	C25	C27	109.72(18)
N4	C4	C5	121.4(2)	C9	C25	C28	110.24(19)
C5	C4	C3	116.8(2)	C27	C25	C26	109.8(2)
C6	C5	C4	121.1(2)	C28	C25	C26	109.3(2)
C5	C6	C1	122.6(2)	C28	C25	C27	108.6(2)
N2	C7	C1	127.72(18)	C12	C29	C30	110.45(18)
N2	C7	C8	107.96(17)	C12	C29	C31	108.58(18)
C8	C7	C1	124.32(18)	C12	C29	C32	110.00(18)
C9	C8	C7	109.73(18)	C30	C29	C32	108.5(2)
C8	C9	C10	105.56(18)	C31	C29	C30	109.4(2)
C8	C9	C25	128.55(19)	C31	C29	C32	109.9(2)
C10	C9	C25	125.87(19)	F1	B1	N2	108.67(16)
N1	C10	N2	124.31(18)	F1	B1	N3	111.23(16)
N1	C10	C9	126.29(18)	F2	B1	F1	109.51(16)
N2	C10	C9	109.38(17)	F2	B1	N2	111.20(17)
N1	C11	N3	123.89(18)	F2	B1	N3	107.71(16)
N1	C11	C12	127.07(18)	N2	B1	N3	108.52(16)
N3	C11	C12	109.00(17)				

Table 6 Torsion Angles for tbu-scy.

A	B	C	D	Angle/°	A	B	C	D	Angle/°
N1	C11	C12	C13	-176.9(2)	C11	N3	C14	C15	-175.79(18)
N1	C11	C12	C29	-1.2(3)	C11	N3	B1	F1	-121.13(18)
N2	C7	C8	C9	0.2(2)	C11	N3	B1	F2	118.85(18)
N3	C11	C12	C13	0.7(2)	C11	N3	B1	N2	-1.6(2)
N3	C11	C12	C29	176.28(18)	C11	C12	C13	C14	0.9(2)
N3	C14	C15	C16	-12.1(3)	C11	C12	C29	C30	175.8(2)
N3	C14	C15	C20	167.74(19)	C11	C12	C29	C31	-64.2(3)
N4	C4	C5	C6	179.0(2)	C11	C12	C29	C32	56.1(3)
N5	C18	C19	C20	-179.2(2)	C12	C13	C14	N3	-2.2(2)
C1	C2	C3	C4	-0.2(3)	C12	C13	C14	C15	176.20(18)
C1	C7	C8	C9	-179.31(19)	C13	C12	C29	C30	-9.5(3)
C2	C1	C6	C5	0.5(3)	C13	C12	C29	C31	110.4(3)
C2	C1	C7	N2	160.5(2)	C13	C12	C29	C32	-129.2(2)

Table 6 Torsion Angles for tbu-scy.

A	B	C	D	Angle/°	A	B	C	D	Angle/°
C2	C1	C7	C8	-20.0(3)	C13	C14	C15	C16	169.8(2)
C2	C3	C4	N4	-179.0(2)	C13	C14	C15	C20	-10.4(3)
C2	C3	C4	C5	1.1(3)	C14	N3	C11	N1	175.58(18)
C3	C4	C5	C6	-1.2(3)	C14	N3	C11	C12	-2.0(2)
C4	C5	C6	C1	0.4(4)	C14	N3	B1	F1	68.1(2)
C6	C1	C2	C3	-0.6(3)	C14	N3	B1	F2	-51.9(3)
C6	C1	C7	N2	-21.5(3)	C14	N3	B1	N2	-172.35(18)
C6	C1	C7	C8	157.9(2)	C14	C15	C16	C17	179.1(2)
C7	N2	C10	N1	177.47(18)	C14	C15	C20	C19	-178.45(19)
C7	N2	C10	C9	-1.3(2)	C15	C16	C17	C18	-0.7(4)
C7	N2	B1	F1	-53.5(3)	C16	C15	C20	C19	1.4(3)
C7	N2	B1	F2	67.2(3)	C16	C17	C18	N5	179.9(2)
C7	N2	B1	N3	-174.55(18)	C16	C17	C18	C19	1.4(4)
C7	C1	C2	C3	177.6(2)	C17	C18	C19	C20	-0.7(3)
C7	C1	C6	C5	-177.5(2)	C18	C19	C20	C15	-0.7(3)
C7	C8	C9	C10	-1.0(2)	C20	C15	C16	C17	-0.7(4)
C7	C8	C9	C25	177.5(2)	C21	N5	C18	C17	16.5(3)
C8	C9	C10	N1	-177.3(2)	C21	N5	C18	C19	-165.0(2)
C8	C9	C10	N2	1.5(2)	C22	N5	C18	C17	-179.7(2)
C8	C9	C25	C26	-118.9(3)	C22	N5	C18	C19	-1.3(3)
C8	C9	C25	C27	120.7(2)	C23	N4	C4	C3	-178.1(2)
C8	C9	C25	C28	1.2(3)	C23	N4	C4	C5	1.7(3)
C10	N1	C11	N3	-1.5(3)	C24	N4	C4	C3	13.6(3)
C10	N1	C11	C12	175.68(19)	C24	N4	C4	C5	-166.6(2)
C10	N2	C7	C1	-179.8(2)	C25	C9	C10	N1	4.2(3)
C10	N2	C7	C8	0.7(2)	C25	C9	C10	N2	-177.06(19)
C10	N2	B1	F1	120.25(19)	C29	C12	C13	C14	-174.62(19)
C10	N2	B1	F2	-119.14(19)	B1	N2	C7	C1	-5.4(3)
C10	N2	B1	N3	-0.8(2)	B1	N2	C7	C8	175.08(19)
C10	C9	C25	C26	59.3(3)	B1	N2	C10	N1	2.4(3)
C10	C9	C25	C27	-61.1(3)	B1	N2	C10	C9	-176.39(17)
C10	C9	C25	C28	179.4(2)	B1	N3	C11	N1	3.0(3)
C11	N1	C10	N2	-1.3(3)	B1	N3	C11	C12	-174.62(16)
C11	N1	C10	C9	177.3(2)	B1	N3	C14	C13	174.27(18)
C11	N3	C14	C13	2.5(2)	B1	N3	C14	C15	-4.1(3)

Table 7 Hydrogen Atom Coordinates (Å×10^4) and Isotropic Displacement Parameters (Å^2×10^3) for tbu-scy.

Atom	*x*	*y*	*z*	U(eq)
H2	1981.01	7130.83	6405.08	42
H3	2538.68	7286.81	8055.06	44
H5	3594.83	4630.22	6917.35	50
H6	3028.72	4487.99	5273.95	48
H8	1269.9	6505.41	5219.28	41
H13	2800.78	3310.97	-641.29	36
H16	3803.98	4217.99	2769.53	51
H17	4729.71	3460.55	2966.82	56
H19	4505.91	1625.77	9.77	40
H20	3587.09	2419.93	-195.9	37
H21A	5639.58	2887.29	2968.56	66
H21B	5976.89	1668.69	2681.5	66
H21C	5368.51	1618.63	3322.2	66
H22A	5281.61	417.07	812.05	68
H22B	5916.25	997.79	970.58	68
H22C	5465.38	1538.02	41.7	68
H23A	3852.66	4428.85	8815.95	75
H23B	4156.55	5453.82	9582.24	75
H23C	4245.26	5433.94	8228.79	75
H24A	3248.12	7554.08	9500.92	73
H24B	3498.47	6526.46	10334.26	73
H24C	2847.4	6432.02	9823.03	73
H26A	514.32	4611.26	2129.45	77
H26B	-99.76	5115.62	2539.22	77
H26C	319.01	4407.49	3420.3	77
H27A	801.79	7767.72	2314.21	68
H27B	208.99	7183.71	1828.35	68
H27C	823.51	6638.2	1468.56	68
H28A	244.15	6217.74	4736.73	76
H28B	-150.49	6891.85	3790.75	76
H28C	430.89	7516.43	4283.93	76
H30A	2106.62	4093.46	-2139.2	71
H30B	1472.38	3548.93	-2403.49	71
H30C	1957.69	2747.03	-1762.15	71
H31A	1317.43	2369.2	-110.8	87
H31B	812.77	3096.09	-776.73	87
H31C	1000.96	3469.95	500.53	87

Table 7 Hydrogen Atom Coordinates (Å×10^4) and Isotropic Displacement Parameters (Å^2×10^3) for tbu-scy.

Atom	*x*	*y*	*z*	U(eq)
H32A	1176.07	5574.84	-151.51	73
H32B	1002.91	5225.4	-1442.57	73
H32C	1621.22	5832.91	-1156.45	73

Refinement model description

Number of restraints - 0, number of constraints - unknown.

Details:

1. Fixed Uiso

At 1.2 times of:

All C(H) groups

At 1.5 times of:

All C(H,H,H) groups

2.a Aromatic/amide H refined with riding coordinates:

C2(H2), C3(H3), C5(H5), C6(H6), C8(H8), C13(H13), C16(H16), C17(H17), C19(H19), C20(H20)

2.b Idealised Me refined as rotating group:

C21(H21A,H21B,H21C), C22(H22A,H22B,H22C), C23(H23A,H23B,H23C), C24(H24A,H24B, H24C), C26(H26A,H26B,H26C), C27(H27A,H27B,H27C), C28(H28A,H28B,H28C), C30(H30A, H30B,H30C), C31(H31A,H31B,H31C), C32(H32A,H32B,H32C)

This report has been created with Olex2, compiled on 2021.12.09 svn.r5202d8cf for OlexSys. Please let us know if there are any errors or if you would like to have additional features.

5 References

1 Y. Guo, Y. Liang, Y. Wang, J. Zhang, C. Wang, Y. Sun, X. Feng and G. Zhao, *Dyes Pigm.*, **2022**, 208, 110791.

2 A. Upadhyay, P. Kundu, V. Ramu, P. Kondaiah and A. R. Chakravarty, *Inorg. Chem.*, 2022, **61**, 1335–1348.

3 W. Zhang, B. Li, H. Ma, L. Zhang, Y. Guan, Y. Zhang, X. Zhang, P. Jing and S. Yue, *ACS Appl. Mater. Interfaces*, 2016, **8**, 21465–21471.

4 Y. Zhang, C. Wen, Y. Liu, A. Li, Q. Guo, X. Zhang, L. Fu, S. Xu, D. Qiao, P. Zheng, W. Zhu and Q. Pan, *Chem. Eng. J.*, 2023, **470,** 144345.

5 W. Wang, Y. Gao, M. Zhang, Y. Li and B. Tang, *ACS Nano*, 2023, **17**, 7394–7405.

6 S. Yao, Y. Chen, H. Xu, F. Qi, Y. Zhang, T. Yang, Y. Wu, H. Fang, W. He and Z. Guo, *Dyes Pigm.*, 2022, **206**, 110583.

7 H. Dang, D. Yin, Y. Tian, Q. Cheng, C. Teng, Y. Xu, and L. Yan, *J. Mater. Chem. B*, 2022, **10**, 5279-5290.

8 L. Gai, R. Zhang, X. Shi, Z. Ni, S. Wang, J. Zhang, H. Lu, and Z. Guo, *Chem. Sci.*, 2023, **14**, 1434-1442.

9 Y. Chu, X. Xu and Y. Wang, *J. Phys. Chem. Lett.*, 2022, **13**, 9564–9572.

10 C. Liu, M. Tian and W. Lin, *J. Mater. Chem. B*, 2020, **8**, 752-757.

11 S. Xu, H. Liu, S. Huan, L. Yuan and X. Zhang, *Mater. Chem. Front.*, 2021, **5**, 1076-1089.

12 M. Shi, X. Liu, W. Pan, N. Li, and B. Tang, *J. Mater. Chem. B*, 2023, **11**, 6478-6490.

13 Y. Xiao, D. Wang, B. Luo, X. Chen, Y. Yao, C. Song, M. Wu, P. Li, X. Li, H. Zhang, X. Zhu, X. Yang and J. Hu, *Nano Today*, 2022, **47**, 101632.

14 H. Bian, D. Ma, X. Zhang, K. Xin, Y. Yang, X. Peng and Y. Xiao, *Small*, 2021, **17**, 2100398.

15 Q. Wang, X. Zhang, Y. Sun, L. Wang, L. Ding, W. Zhu, W. Di and Y. Duan, *Biomaterials*, 2019, **212**, 73-86.

16 H. Ge, J. Du, S. Long, X. Xia, J. Zheng, N. Xu, Q. Yao, J. Fan and X. Peng, *Adv. Healthcare Mater.*, 2021, **11**, 2101449.